

## Correction on school geometry and density: approach based on acoustic image simulation

Noël Diner\*

TMSI/TP, Ifremer centre de Brest, BP 70, 29280 Plouzané cedex, France

Received 12 July 2000; accepted 26 March 2001

---

**Abstract** – Models of simulated schools have been used to determine the intrinsic variability in echotracés due to beam pattern effect. This work concerns only morphometric and energetic parameters that can be extracted from echotracés. It appears that  $dST$ , the difference between school density and processing threshold is a key parameter, which directly influences the concerned detection angles. Relations, taking into account  $dST$  but also,  $Nb_1$ , the relative school length image compared to the beam width, have been settled for the calculation of length and density corrections. In most cases, corrected values are obtained with errors less than respectively 5% for length and 0.5 dB for density (reverberation index), provided that the  $Nb_1$  value is 1.5 or more. When  $Nb_1$  is less than 1, it seems impossible to bring some pertinent corrections. The school energy does not need any correction. It is recommended to use threshold values not too low, to avoid detection through the side lobes. However this setting must be determined in order to obtain  $dST$  values greater than 10 dB. Thresholds between  $-60$  and  $-65$  dB seem adequate, at least for schools volume backscattering strength (VBS,  $S_v$ ) values commonly encountered in the Bay of Biscay.  
© 2001 Ifremer/CNRS/Inra/IRD/Cemagref/Éditions scientifiques et médicales Elsevier SAS

acoustic / fish detection / fish schools

**Résumé** – Correction de descripteurs géométriques et énergétiques extraits de bancs de poissons : approche basée sur de la simulation d'images acoustiques. Une analyse de la variabilité des descripteurs extraits des échos de bancs de poissons a été effectuée en tenant compte des différents paramètres qui conditionnent l'image acoustique obtenue grâce au sondeur vertical : performances et caractéristiques du sondeur vertical, taille et densité du banc, seuil de traitement. Une simulation des échos permet de comparer les valeurs réelles et « image » des descripteurs. Un algorithme original de correction est proposé. Il concerne uniquement les descripteurs morphologiques et énergétiques que l'on peut extraire des échos de bancs de poissons. Le paramètre clé pour ces corrections est la différence,  $dST$ , entre le seuil de traitement des données et l'index de réverbération du banc concerné. Pour des images simulées, ce paramètre permet d'obtenir des valeurs corrigées, avec par exemple des erreurs inférieures à 5% pour la longueur ou 0,5 dB pour l'index de réverbération de volume, pourvu que le banc ait une taille suffisante par rapport au faisceau d'émission du sondeur. Les limites de ces corrections sont également étudiées. Des seuils de traitement compris entre  $-60$  et  $-65$  dB semblent les mieux adaptés, du moins pour le type de bancs rencontrés dans le golfe de Gascogne.  
© 2001 Ifremer/CNRS/Inra/IRD/Cemagref/Éditions scientifiques et médicales Elsevier SAS

acoustique / détection de poissons / banc de poissons

---

### 1. INTRODUCTION

For some years, an increasing interest has arisen in acoustic image analysis to carry out automatic classification on the detected echotracés (Souid, 1988; Scalabrin, 1997). Such classification is important as it may allow direct acoustic stock evaluation, species by species and school by school. This can be compared

with the classical method, which produces a global biomass evaluation that must be split into its different specific components, for instance by using catch results.

Nevertheless, due to a poor resolution of the measurement tool – the vertical echosounder – the same image may reflect different field situations or, alternatively, the same kind of fish concentration may pro

\*Correspondence and reprints: fax: +33 298 224 650.  
E-mail address: noel.diner@ifremer.fr (N. Diner).

duce various images. Without appropriate corrections of the descriptors extracted from the acoustic images, classification would be quite inaccurate.

In the past, some authors (Olsen, 1969; Johannesson and Losse, 1977) have proposed school size (and size-dependent) corrections based only on nominal beam opening. In practical situations, on a great number of schools, the inaccuracy of this type of correction was clearly demonstrated. Threshold dependency of effective detection angle has also been demonstrated (Aglen, 1982) and it appears that any correction algorithm must consider this parameter.

This work is dealing only with vertical echosounder traces whose horizontal dimensions suffer from beam effect distortion (Reid, 2000). It first describes in details an algorithm established for school descriptor correction based on echotrace simulation. As this kind of simulation cannot perfectly reflect the field variability, algorithm corrections have then been operated on real school detection.

## 2. METHODS: CORRECTION ALGORITHM BASED ON ECHOTRACE SIMULATION

Simulation of acoustic school images seems to be a necessary step when establishing this kind of algorithm, since it is the only situation where both real school and corresponding image echotrace are well known. An algorithm can be established by comparing descriptor values extracted from both situations.

### 2.1. Approach to the problem

The resolution of vertical echosounders is defined by its confusion volume, which is determined by the pulse duration and, at a given depth, by the beam width. As the acoustic sampling unit is a volume relatively large compared to the size of fish schools, the processed acoustic image of a school is a poor representation of its actual size, shape and density. The vertical echosounder acts like a distortion filter and:

- the section length of the school image is increased by a value depending on the basic angle value of the directivity function but also on the school depth (*figure 1*),

- the average fish density computed from the acoustic school image is systematically underestimated: intensity values of unfulfilled pings, at the beginning and at the end of the school detection (where confusion volumes are not entirely filled up with fish), are used together with those of fulfilled pings, at the centre of the school, to compute the average density. Of course, other descriptors like area, perimeter, energy, which are correlated to length and density, may also be affected by some systematic errors or bias.

The effective detection angle is an important factor, which must be taken into account, since, due to the directivity function of a transducer, targets with a high target strength (*TS*) are: 1) effectively sampled with a larger beam angle, and 2) also sampled by more pings.

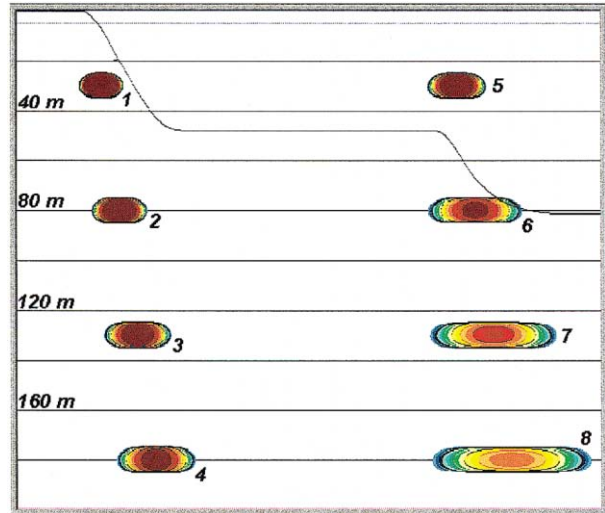


**Figure 1.** Simulated echotrace of the same school. Length: 20 m and  $S_v$ : -35 dB at different depths (30, 80, 130 and 180 m) for two nominal beam angles: 5° on the left (schools 1 to 4) and 15° on the right (schools 5 to 8). The different colour rings surrounding the traces are a reflection of lower echo levels when the school does not occupy the whole beam (unfulfilled pings). For 15° at a depth higher than 100 m, no ping contains echo levels (brown colour) reflecting the real volume backscattering strength of the school.

The parameter affecting the effective detection angle is not only  $S_v$ , the school volume backscattering strength (VBS), but the difference between  $S_v$  and  $Th$ , the processing threshold.

Due to the directivity function, the effective detection angle varies continuously according to the difference between density and threshold. For instance, a high threshold excludes from analysis the lower amplitude values that surround the school image (*figure 1*), producing a decrease in the apparent school image length.

Three different angles concerning this problem can be defined (*figure 2*):

- $\theta$ , the nominal angle determined by the directions for which a 6 dB attenuation (two ways) is observed compared to the on-axis sensitivity level.
- $B$ , the detection angle defined as the top angle of the cone including all the fish contributing, at a given time, in the echo amplitude. This angle depends on the difference between the mean school density and the processing threshold.
- $A$ , the ‘attack’ angle defined as the angle between a vertical line, from the transducer, and another line, towards the school edge, measured at the moment when the school detection is just beginning. This happens when the number of fish, within the acoustic beam, is high enough to produce an echo signal amplitude just above the processing threshold. The school length increase,  $dL$ , is directly related to this angle:

$$dL = 2 \times P \times \tan (A/2)$$

where  $P$  is the mean school depth.

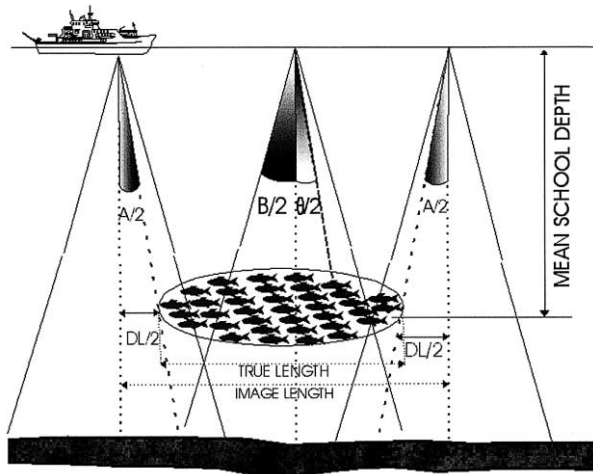


**Figure 2.** Different angles involved in school detection.  $\theta$ : nominal beam opening, defined by the 6 dB attenuation (two way);  $B$ : detection angle of the cone inside which are included all the fish contributing at the echo level;  $A$ : attack angle that must be used for  $dL$ , length correction of echotraces.

The two first angles,  $\theta$  and  $B$ , depend on the directivity function of the transducer.  $B$  is also related to the difference between school backscattering strength and processing threshold. Estimating the value of these angles would seem quite straightforward. This is not really the case for the third angle, which is mostly determined by fish density located in a border zone of the acoustic beam. Simulations of acoustic school images, based on a priori well-known configuration of schools, might provide a general expression allowing to estimate the attack angle by taking into account all relevant parameters.

## 2.2. Description of the acoustic simulator

Vertical echosounder image simulator was developed in part to explain the variability in descriptor values which are extracted from school images by the software MOVIESB, developed over many years by Ifremer (Weill et al., 1993). The simulator software is developed for PC computer applications (Diner and Scalabrin, 1997). All the parameters required for image construction can be defined for a given simulation:

- different species, for each of them:  $TS$  relation and weight/length characteristics,
- performances and settings of the echosounder,
- settings for display: range, absolute threshold in decibels and colour dynamic,
- up to ten different schools with, for each: length, width and height, species (length and density), position in the water column along the vessel route (depth and distance), right under the transducer or some metres outside. The shape of all these schools is ellipsoidal and the density inside the school is uniform.

Using all these parameter values, it is possible to obtain:

- an image of the real situation, displayed on the computer screen with the same scales as on the echosounder, depending on vessel speed and ping rate,
- a file with most of the school MOVIESB descriptors, calculated for the real situation,
- a simulated image of the school echoes, this simulation takes into account the directivity function of the transducer (rectangular shape only),
- a file, of the same format as MOVIESB, of this simulated acoustic image. It becomes thus possible to process this kind of file in order to extract, from the simulated images, the different descriptors and allows comparison of image and real values.

## 2.3. Processed simulated data

The variability in school descriptor values, extracted from acoustic images, depends on several parameters (cf. supra), mainly: beam angle, school dimensions, density and depth. Simulations have been performed on a main set of six schools, whose characteristics, a priori defined, are presented in *table I*.

Some other schools have also been simulated to verify the stability of some relations against morphological parameter variation.

These values of school size and density have been chosen to include the main population of descriptors encountered in the school data bank gathered in the Bay of Biscay over more than 10 years.

The depth of each school has been systematically determined to be 30, 80, 130 and 180 m. For the simulation, these schools have been put exactly under the vessel track, but at random distance. Some variability in school image descriptors has thus been obtained.

To cover most of the used equipment variability, four different beam angles have been simulated: 5, 7.5, 10 and 15°. The pulse duration was fixed at 1 ms and the acoustic performances have been varied so as to obtain, in each case, the same echosounder constant,

**Table I.** Main characteristics of the schools used for simulation.

Type	$L_s$ (m)	$W$ (m)	$H$ (m)	$Sv_s$ (dB)	Volume (m <sup>3</sup> )	Weight (kg)
A3	20	20	10	-35	2 096	896
A4	20	20	10	-45	2 096	90
B3	50	50	10	-35	13 100	5 601
B4	50	50	10	-45	13 100	560
C3	100	100	20	-35	104 800	44 808
C4	100	100	20	-45	104 800	4 481

The simulated species is sardines (target strength of a single fish inside the school,  $TS = -48$  dB).  $L_s$ : length of the school, along the vessel track;  $H$ : height of the school;  $W$ : width of the school, perpendicular to the vessel track;  $Sv_s$ : volume backscattering strength of the school.

which represents the acoustic performance of the equipment; it is defined by the relation:

$$C_s = - \left[ (Sl + Vr) + 10 \log \psi + 10 \log \frac{c\tau}{2} \right]$$

with:

- $(Sl + Vr)$ : source level plus voltage response,
- $10 \log \psi$ : equivalent beam angle,
- $\tau$ : pulse duration,
- $c$ : sound speed.

Vessel speed and ping rate were fixed respectively at 5 knots,  $2 \text{ pings}\cdot\text{s}^{-1}$  for ranges down to 100 m, and 2.5 knots,  $1 \text{ ping}\cdot\text{s}^{-1}$  for ranges between 100 and 200 m. These settings give  $e$ , a constant interping distance of 1.3 m.

All simulated images have been processed by MOVIESB, over a range of  $Th$  values of:  $-65.1$ ,  $-55.1$ ,  $-51.1$ ,  $-48.1$ ,  $-45.1$ ,  $-41.1$ ,  $-38.1$  and  $-35.1$  dB. These values, combined with the  $Sv$  of the different schools, give possible differences  $dST = Sv - Th$  of:  $30.1$ ,  $20.1$ ,  $16.1$ ,  $13.1$ ,  $10.1$ ,  $6.1$ ,  $3.1$  and  $0.1$  dB.

The maximum  $dST$  value studied is thus  $30.1$  dB. Higher values were not used, because, when considering the transducer directivity function, they could induce detection angles high enough to include the secondary lobes.

An important data set (more than 700 school situations) has thus been obtained, giving a good idea of the phenomenon variability. For example, substantial changes can be seen in both the acoustic image school length and reverberation index (figure 3). This is dependent on beam width, school depth, but also on  $dST$ , which appears to be a key parameter when corrections of the descriptors are required.

## 2.4. Problem analysis

The complexity of examining the different analysed biases concerns many parameters. This made extracting general relations difficult. As the  $dST$  is one of the keys and as  $Th$  is known, it is necessary to focus on the parameter  $Sv$ . The bias, done on this descriptor value extracted from the school image, is related to the ratio between fulfilled and unfulfilled pings (figure 2), i.e. the school length compared to the beam width. A standardisation of the image length by the beam width at the school depth allows the possibility of processing together all the data, whatever the school length and depth or nominal beam opening. Establishing general variation laws appears then easier by using the normalised school dimension in terms of beam width number,  $Nb$ .

This data set indicates a close relationship between the angles  $A$  and  $B$  and the key  $dST$  values. This is especially the case when using  $Sv_r$ , true VBS of the considered school, when calculating  $dST$ . However, only  $Sv_i$ , the image value that can be extracted from the echotracés, is known with a systematic bias.

For this reason, an approach composed of three steps has been considered:

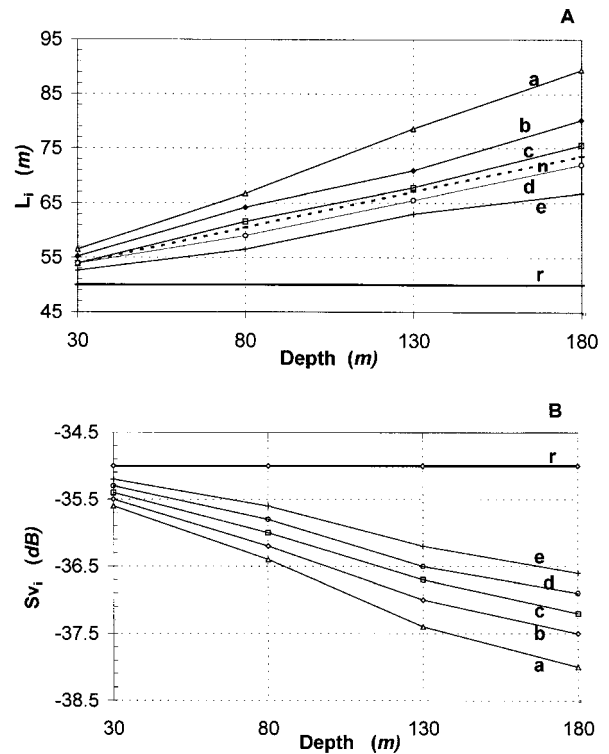


**Figure 3.** Simulated echotracés characteristics using a nominal angle  $7.5^\circ$ , for a school length of 50 m and  $Sv_r$  of  $-35$  dB, and several  $dST$  values: **a** ( $\Delta$ ):  $30.1$  dB; **b** ( $\diamond$ ):  $20.1$  dB; **c** ( $\square$ ):  $16.1$  dB; **d** ( $\circ$ ):  $13.1$  dB; **e** ( $+$ ):  $10.1$  dB. **A.** Echotrace length,  $L_i$ , versus mean school depth. Dotted line (**n**) reflects theoretical length, calculated by using the nominal angle. **B.** Echotrace volume backscattering strength,  $Sv_i$ , versus mean school depth.

- Step 1: determine with the highest possible accuracy  $Sv_p$ , a temporary value for the VBS. This leads to the possibility of computing  $B_p$ , a first detection angle used for calculating  $Nb_p$ , the number of beam widths corresponding to the school image.
- Step 2: compute the attack angle  $A$  that allows the definitive corrections of the school length and reverberation index. The school height is only corrected for the pulse duration effect ( $c\tau/2$ ) as the simulator does not take into account the multiscattering effect inside the schools.
- Step 3: process corrections for area, perimeter and energy.

## 2.5. Suggested algorithm

Algorithm expressions can include the following subscripts:

- $r$ : the parameter values of the real school as defined for the simulation,
- $i$ : the values concerning descriptors extracted directly from the acoustic image,
- $c$ : descriptors values after correction,

–  $p$ : temporary values appearing only in the first phase of the algorithm.

**2.5.1. Step 1**

2.5.1.1. Calculate the difference

$$dST_i - Th$$

2.5.1.2. Calculate a detection angle

$$B_i = 0.44 \times \theta \times (dST_i)^{0.45}$$

This relation is an approximate inverse relation of the directivity function of the transducer. It fits quite well with the true function for attenuation range between 0 and 30 dB, which are those concerned by the present study.

2.5.1.3. Calculate a normalised length in terms of beam width number

$$Nb_i = \frac{L_i}{2 \times P_i \times \tan(B_i/2)}$$

where  $P_i$  is the mean depth of the echotrace.

2.5.1.4. Calculate a raw correction for the image VBS

$$dSv_i = 2.56/(Nb_i - 1)$$

This relation has been found by processing, for all the simulated data (all schools and beams at any depths and random horizontal distance), the parameters  $Nb_i$  and  $dSv_i$ . It is the best fitting relation and an asymptotic value is observed for  $Nb_i = 1$ .

2.5.1.5. Calculate a temporary VBS

$$Sv_p = Sv_i + dSv_i$$

2.5.1.6. Calculation of the corresponding difference

$$dST_p = Sv_p - Th$$

**2.5.2. Step 2**

2.5.2.1. Compute the attack angle

$$A_c = \theta \times [1.04 \times (dST_p)^{0.33} - 1.52]$$

As for  $dSv_i$ , this attack angle relation is the best fitting equation when processing all the simulated data. This relation gives a 0° angle when  $dST_p$  is equal to 3.18 dB, which means that the school then occupies a little less than half of the acoustic beam. At this particular point, the transducer is just on the vertical line of the school edge.

2.5.2.2. School length correction

$$L_c = L_i - 2 \times P_i \times \tan(A_c/2)$$

This angular correction becomes very large when school depth and difference,  $dST$ , are high. In some cases when the  $dST$  value is lower than 3.18 dB, the angle  $A$  becomes negative and the school image length is smaller than the true length.

2.5.2.3. Calculate a new school length, normalised in term of beam width

$$Nb_c = \frac{L_c}{2 \times P_i \times \tan(A_c/2)}$$

In this step, the attack angle, which is known, has been used instead of the detection angle  $B$ . It would seem preferable as it allows, for a specific school, a better ratio between fulfilled and unfulfilled pings, a ratio that directly influences the bias on  $Sv$ .

2.5.2.4. New correction of the VBS

$$dSv_c = 4.09/(Nb_c)^{0.88}$$

by the updated relation, which was established using the whole simulated data set. For negative values of the angle  $A_c$ , when  $dST_p$  is less than 3.18 dB,  $Nb_c$  is also negative and the calculation of  $dSv_c$  becomes impossible. It can be observed that, in this special case due to low values for  $dST$ , the  $Sv$  values are very close to the true one and no correction is required.

2.5.2.5. Calculation of the corrected VBS

$$Sv_c = Sv_i + dSv_c$$

**2.5.3. Step 3**

2.5.3.1. Correction of the height

$$H_c = H_i - c\tau/2$$

2.5.3.2. Correction of the area

$$S_c = S_i \times (L_c \times H_c)/(L_i \times H_i)$$

2.5.3.3. Correction of the perimeter

$$Pr_c = Pr_i(L_c + H_c)/(L_i + H_i)$$

2.5.3.4. Calculation of the corrected energy

$$En_c = En_i \times \frac{S_c}{S_i} \times 10^{\frac{dSv_c}{10}}$$

This relation is established taking into account that the school energy is the product of its area by a factor equivalent to the mean square amplitude, term equal to the antilog of the VBS.

**3. RESULTS**

By operating this algorithm on the image descriptors of the set of simulated schools it appears that:

– The final corrected values for length are very close to the true values: relative errors less than 2% are very common, this correction being independent of the nominal beam angle or school depth. A slight variation (approximately 1%) is observed according to the nominal *dST* value (figure 4). However, significant errors can appear when the school size, expressed in term of beam width, is decreasing. This point is examined later.

– The corrected VBS values,  $Sv_c$ , are very close to true ones: the difference is less than 0.3 dB in most of the studied cases. However, as for school length, increasing errors are observed when the school size is decreasing (figure 5).

– With regards to the area and perimeter, the corrected values reach the same accuracy than for length. For the energy corrections, which sum the errors on surface and reverberation index, the results are not at the level of those observed for length and index (figure 6). It appears thus unnecessary to correct this parameter.

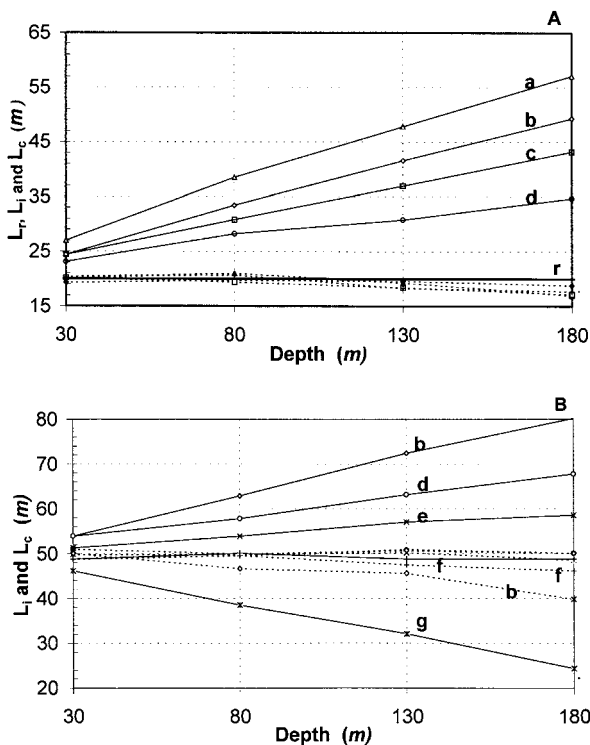


**Figure 4.** Echotrace lengths and corresponding corrected values (dotted lines) versus mean school depth, using a 7.5° nominal angle, for various *dST*: a ( $\Delta$ ): 30 dB; b ( $\diamond$ ): 20 dB; c ( $\square$ ): 16 dB; d ( $\circ$ ): 10 dB; e ( $\times$ ): 6 dB; f (+): 3 dB; g ( $\ast$ ): 0.1 dB. A. For a school  $L_r$  of 20 m and  $Sv_r$  of -35 dB. B. for a school  $L_r$  of 50 m and  $Sv_r$  of -45 dB. In this last example, a *dST* of 3 dB produces echotrace lengths very close to real ones; for a *dST* of 0.1 dB, the attack angle being negative, the echotrace lengths are less than the real ones, but the corrected values are not very different from the true ones.

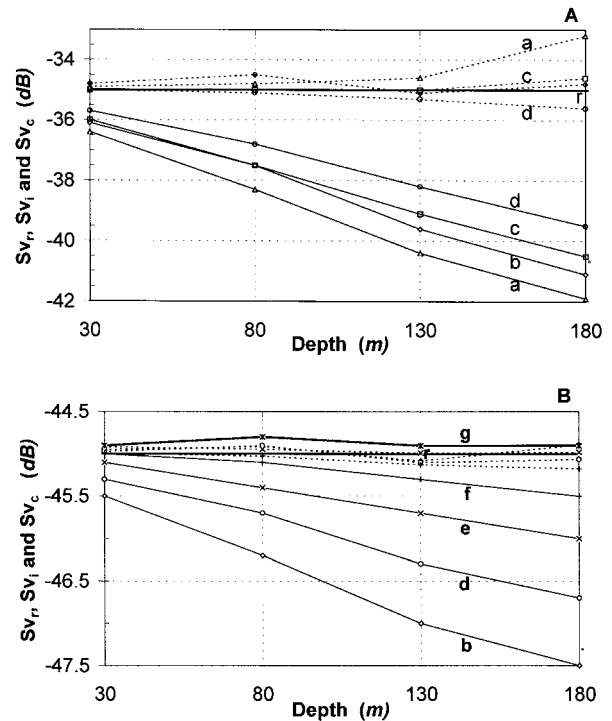


**Figure 5.** Volume backscattering strength and corresponding corrected values (dotted lines) versus mean school depth, using a 7.5° nominal angle, for various *dST*: a ( $\Delta$ ): 30 dB; b ( $\diamond$ ): 20 dB; c ( $\square$ ): 16 dB; d ( $\circ$ ): 10 dB; e ( $\times$ ): 6 dB; f (+): 3 dB; g ( $\ast$ ): 0.1 dB. A. For a school  $L_r$  of 20 m and  $Sv_r$  of -35 dB. B. For a school  $L_r$  of 50 m and  $Sv_r$  of -45 dB. For greater depths (e.g. 180 m), there are still significant errors on the corrected values for the 20 m school (A). When the attack angle is negative, (*dST* = 0.1 dB in B), the image values are not very different of the true ones (r), and there is no great incidence if in this case the correction is not possible.

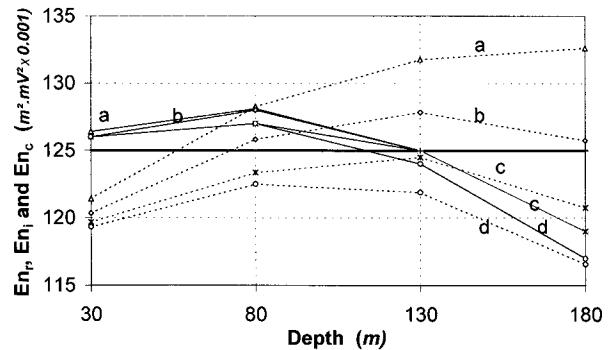


**Figure 6.** Real image and corrected energies versus mean school depth, using a 7.5° nominal angle, for a school length of 50 m and  $Sv_r$  of -35 dB. Some variability appears for the image calculated energies (continuous lines). The corrected values (dotted lines) are not uniformly better than the image ones.

### 3.1. Limitations

The limitations of this kind of correction have also been studied. For this purpose, simulations of two other schools, smaller than those studied above, have been conducted. The main characteristics of these schools are: length: 14 m, width: 20 m, height: 6 m,  $S_v$ : -35 and -45 dB.

The simulations were done with the same echosounder parameters and then processed by MOVIESB, with the same thresholds as above. These schools have been placed every 20 m depth between 20 and 180 m. For a nominal angle of 5°, the parameters of these schools are quite well corrected for all depths  $P$ . However, in the case of a nominal angle of 10° and a  $dST$  of 6.1 dB, the algorithm gives inaccurate corrections for depths greater than 140 m. For high  $dST$  values and wide beam angles, for example 30 dB and 15°, the corrections become inaccurate for depths over 100 m. Expressed in term of beam width, the limitations of this algorithm appear more clearly (figure 7):

- for  $Nb_i$  values above 2,  $S_v$  is corrected with differences less than 0.5 dB and the maximum relative error for length is 10%,
- for  $Nb_i$  values under 2, the error levels increase rapidly; there is an asymptotic value for  $Nb_i$  equal to 1.

Thus, the limitation for using this algorithm appears to be for schools whose relative dimension of  $Nb_i$  is approximately equal to 1.5.

The detection and attack angles defined above are directly dependent on  $dST$ , the difference between school VBS and processing threshold. While the threshold, determined by the operator, is well known, this is not the case of VBS. Only an image-based value of this parameter is known. This value can be subject to substantial errors (e.g. low  $Nb_i$  values). Thus it appears interesting to calculate for the angle  $A$  the error induced by a systematic error of 1 dB when determining  $S_v$ . This has been studied for  $dST$  values between 0 and 30 dB (figure 8).

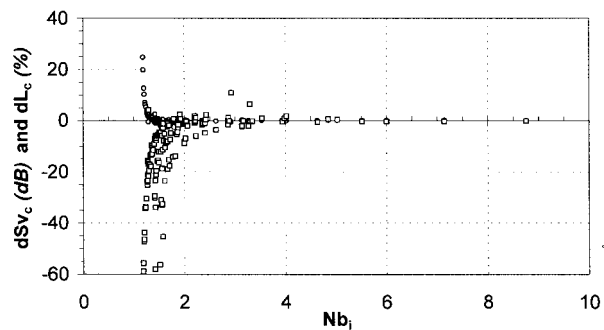


**Figure 7.** Plot versus  $Nb_i$  values, of many values for the differences  $dSv_c (= Sv_c - Sv_r)$  and school length relative errors,  $dL_c$ , (in percent). For  $Nb_i$  above 2, the errors are generally low. For  $Nb_i$  below 1.5, a significant increase of inaccuracy is observed for corrected values. There is an asymptotic value for  $Nb_i = 1$  and 1.5 seems the lower acceptable limit for operating the proposed correction algorithm.

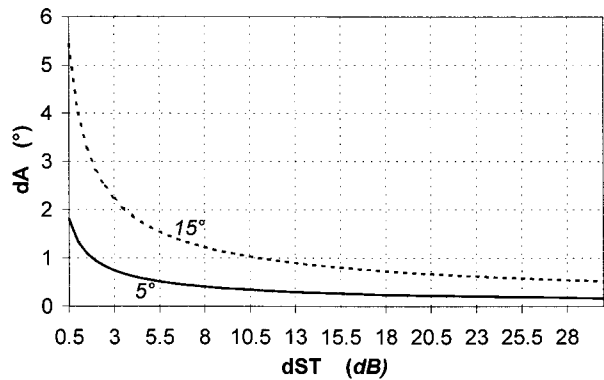


**Figure 8.** Error done on the attack detection angle,  $A$ , versus  $dST$  for a constant potential error of 1 dB when determining the difference  $dST$ . Curves are plotted for two nominal angles: 5° (continuous line) and 15° (dotted line). The errors are minimal for  $dST$  values above 10 dB: in this part of the transducer directivity function, a given variation of  $dST$  induces a minimal angle change.

Roughly speaking, when  $dST$  is less than 3 dB, the angular error increases rapidly: in this case, concerning only the central part of the acoustic beam, the angle values are small and the relative error becomes more important. Inversely, for  $dST$  values between 10 and 30 dB, the angular errors are reduced. This seems thus the best field for operating analysis on school descriptors. As the average  $S_v$  of the schools encountered in open sea seems to stand between -45 and -35 dB, a threshold value of -60 or -65 dB will give the best chance of precision.

### 3.2. Effect of ping rate

The simulated images, studied above, have been obtained by using a constant ping interval,  $e$ , of 1.3 m (cf. 4. practical application). This ping interval effect may also affect the image length by supplementary errors, as this length is determined at  $\pm e$ . This parameter can be computed by:

$$e = (1852 \times V_N) / (3600 \times p),$$

with  $V_N$ , vessel speed in knots, and  $p$ , ping rate in number per second.

Typically this means an error of  $\pm 5.1$  m when, for instance, the vessel speed is 10 knots, on 200 m water depth, and operating a ping rate of  $1 \text{ s}^{-1}$ . The variation in school length on the echotrace is equal to the ping interval. Of course, the relative supplementary error that will affect the length decreases with depth for the image. However, after correction by the algorithm, the error in school length remains roughly the same as the relative ping error compared to the real school length. Concerning the VBS, a combined effect of length variation of echotrace and relative small dimension of school (low  $Nb_i$  values) may increase the variation of the corrected  $S_v$ .

Therefore, it appears important to operate echosounders with low value for  $e$ , i.e. the highest ping rate allowed by the detection range and, when necessary, a reduced vessel speed.

### 3.3. Discussion

By using acoustic image simulation, which allows the comparison of descriptor values extracted from acoustic images and real situations, it has been possible to produce an algorithm for correcting many parameters whose errors are mainly due to the beam pattern effect.

However, the database used to develop the correction algorithm are composed of schools with a particular shape (ellipsoid) and, in addition, with a uniform density. Even if these schools have been placed at a random distance on the simulated vessel track, this is certainly not a perfect reflection of field situations, where many fluctuations concerning echotrace shape and internal density are observed.

The simulation takes into account the directivity function of the transducer, which is required to obtain precise information on the different detection angles. However, only rectangular transducers have been used thus far for image simulation. In the case of circular transducers, there are some differences, for instance for the nominal angle, which would be slightly larger, or for the secondary lobe level, about 4 dB lower. However we think that this does not have a major impact on the main conclusions of this work and the proposed algorithm.

The energy descriptor of the schools can be considered as the product of school area by mean squared echo amplitude. For this parameter, the proposed corrections do not appear to be very efficient. This is mainly due to the cumulative effect of errors in the correction of both area and  $S_v$ . In all cases, it does not appear to be necessary to correct the image energy value. It must be emphasised that this kind of descriptor, concerning only a school of limited dimensions, must be considered differently from the same kind of parameter calculated for the purpose of echointegration and stock evaluation. In this case, there is no evaluation bias, as it is only a sampling of the water column that is done.

Nevertheless, if the school image dimensions are large enough compared to the beam width ( $Nb_1 \geq 1.5$ ), the proposed algorithm gives corrected descriptor values with low relative errors. Any classification based on school morphological or energetic descriptors will be improved if this type of correction is previously undertaken. Indeed, depending for instance on echosounder characteristics or school depth, there may be a very significant difference between image and real values. A school image length increase versus depth may be very significant: for example up to 40 m at 200 m with a  $dST$  of 30 dB and a nominal beam angle of  $7.5^\circ$ . Without any previous correction, it seems difficult to compare different echotracés and try to operate advanced classification.

It is also recommended to use processing threshold values high enough to avoid possible detection through the side lobes. However, this setting must be determined for obtaining  $dST$  values greater than 10 dB. Thresholds between  $-60$  and  $-65$  dB seem adapted at least for school VBS values commonly encountered in the Bay of Biscay (Scalabrin and Massé, 1993; Scalabrin, 1997).

## 4. PRACTICAL APPLICATION ON ACTUAL SCHOOL DETECTION

It seems necessary to operate the algorithm on school real detection in order to control the validity of the different corrections on field echotracés with more variability, especially concerning shape and internal density. This exercise has been conducted on schools detected simultaneously by two echosounders with different directivities: the corrected descriptors would have the similar values.

Operating simultaneously, without mutual interference, echosounders with most different directivities is possible, provided that these equipment have quite spaced frequencies. This has been done on R.V. *Thalassa*, using the following echosounders processed simultaneously by MOVIES+ software:

- frequency: 38 kHz, nominal beam angle:  $5.7^\circ$ , pulse duration: 1 ms,
- frequency: 12 kHz, nominal beam angle:  $16^\circ$ , pulse duration: 1 ms.

These echotracés have been processed using the same absolute threshold:  $-60$  dB.

Algorithm tests have been conducted on two sets of detection:

- relatively large echotracés, standing at a mean depth of 140 m (horse-mackerel),
- smaller echotracés at a mean depth of 45 m (sardine).

### 4.1. Large schools

The difficulty in this case, working on quite deep detection, is to make sure that the comparison concerns exactly the same echotracés. Due to its poor angular resolution, the 12 kHz beam ( $16^\circ$ ) induces a coalescing effect on different aggregations, which appears separated using narrower beam ( $5.7^\circ$ ). This was the case for many of the available data (i.e. deep and high school abundance) (figure 9). There are also very different areas covered by the two echosounders on the axis perpendicular to the vessel track. For this group of echotracés, the main characteristics are summarised in table II.

Special attention has been paid into selecting the echotracés for comparison. However, when looking at the echotracés lengths for example, it seems that the compared length variations, between 38 and 12 kHz, for schools No. 33, 28 and 41 are not normal (figure 10).



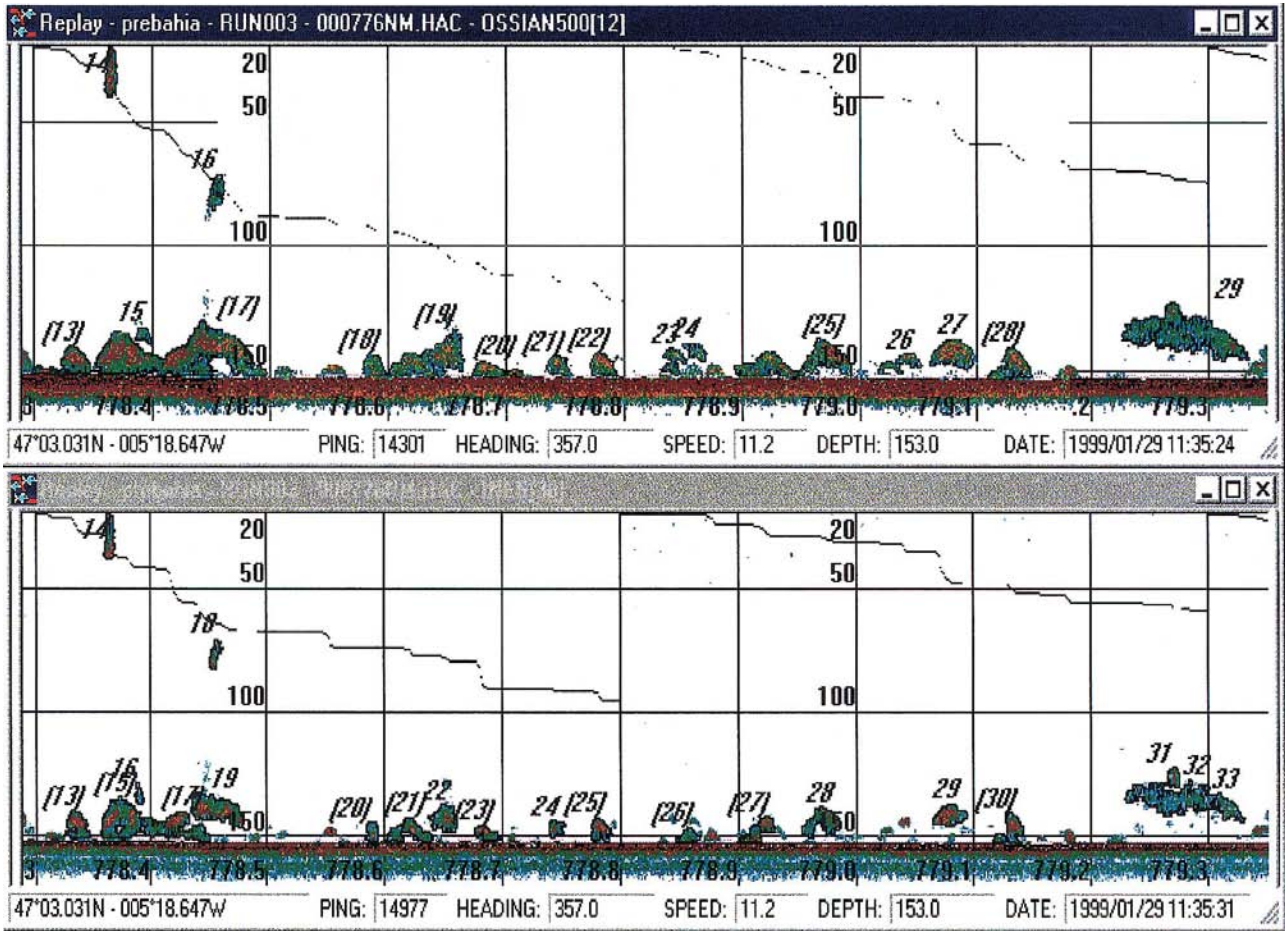


**Figure 9.** Compared echotracés at 12 kHz and 16° nominal angle (upper part) and 38 kHz and 5.7° nominal angle (lower part) obtained on large echotracés of horse-mackerels. On 12 kHz, schools No. 17, 19, 25 and 29 are obviously aggregations of several ones.

**Table II.** Main characteristics of the horse-mackerel schools used for testing the algorithm.

Frequency (kHz)	Beam (°)	Sv <sub>i</sub> (dB)		dST (dB)		Length (m)		Nb <sub>i</sub>		Corrections			
		min	max	min	max	min	max	min	max	Length (m)		Sv (dB)	
										min	max	min	max
12	16	-53.3	-43.5	6.7	16.5	32.1	231	1.25	4.4	9.0	62.5	0.77	14.0
38	5.7	-53.7	-42.1	6.3	17.9	27.6	181	1.63	11.7	3.1	17.7	0.26	4.2

In table III, it can be noticed that some corrections are relatively high and correspond in many cases to the lower values of the factor Nb<sub>i</sub>. However, for schools at a mean depth of 140 m, detected by a 16° nominal beam, the length correction may reach 40 m for an Nb<sub>i</sub> value of 4. Concerning the same echotracés, detected by a 5.7° beam, the corresponding mean corrections are between 10 and 15 m for Nb<sub>i</sub> values around 5.

In this example too, the corrections seem better for length than for Sv. Concerning length (figure 10), corrections are fine for No. 16 and 14, the two schools standing in middle water, and generally acceptable for the others, except 33, 41 and 31. However these last

schools appear not homogeneous in density. Concerning Sv (figure 11), there are some important differences: for example more than 3 dB for No. 48, 10 and 42. The best results (difference between frequencies < 1.3 dB) are observed for the middle water echotracés (No. 16 and 14) and for other schools even if they appear inhomogeneous: for example No. 46, 27, 2 and 33.

**4.2. Small schools**

The corrections become inaccurate when the echotracés dimensions are too small compared to the

**Table III.** Main characteristics of the small schools processed.

Frequency (kHz)	Beam (°)	$Sv_i$ (dB)		$dST$ (dB)		Length (m)		$Nb_i$		Corrections			
		min	max	min	max	min	max	min	max	Length (m)		$Sv$ (dB)	
12	16	-47.7	-33.5	12.9	26.5	8.8	25.5	1.03	1.84	4.3*	21.0*	3.5*	15.9*
38	5.7	-51.8	-26	8.2	34.0	2.3	12.0	1.33	4.1	1.55	7.6	0.3	4.2

\* Corrections among the schools for which corrections were possible.

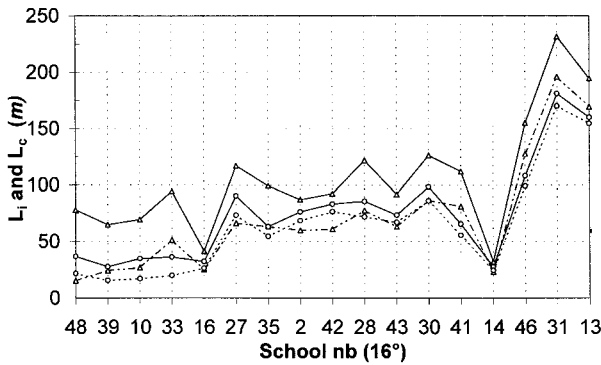


**Figure 10.** Compared length corrections (dotted lines) on large schools, for nominal beam angles 5.7° (○) and 16° (△). School numbers are related to the 12 kHz echogram.

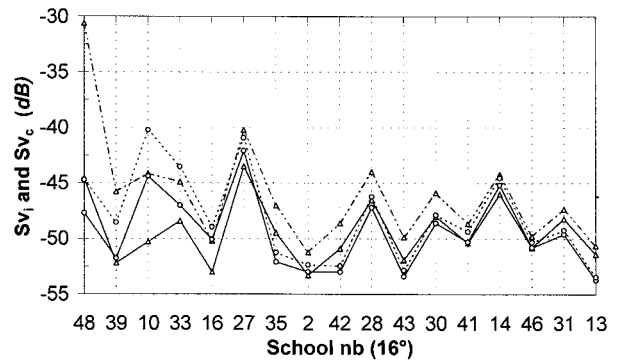


**Figure 11.** Compared volume backscattering strength image (continuous lines) and corrected (dotted lines) for large schools and nominal beam angles 5.7° (○) and 16° (△).

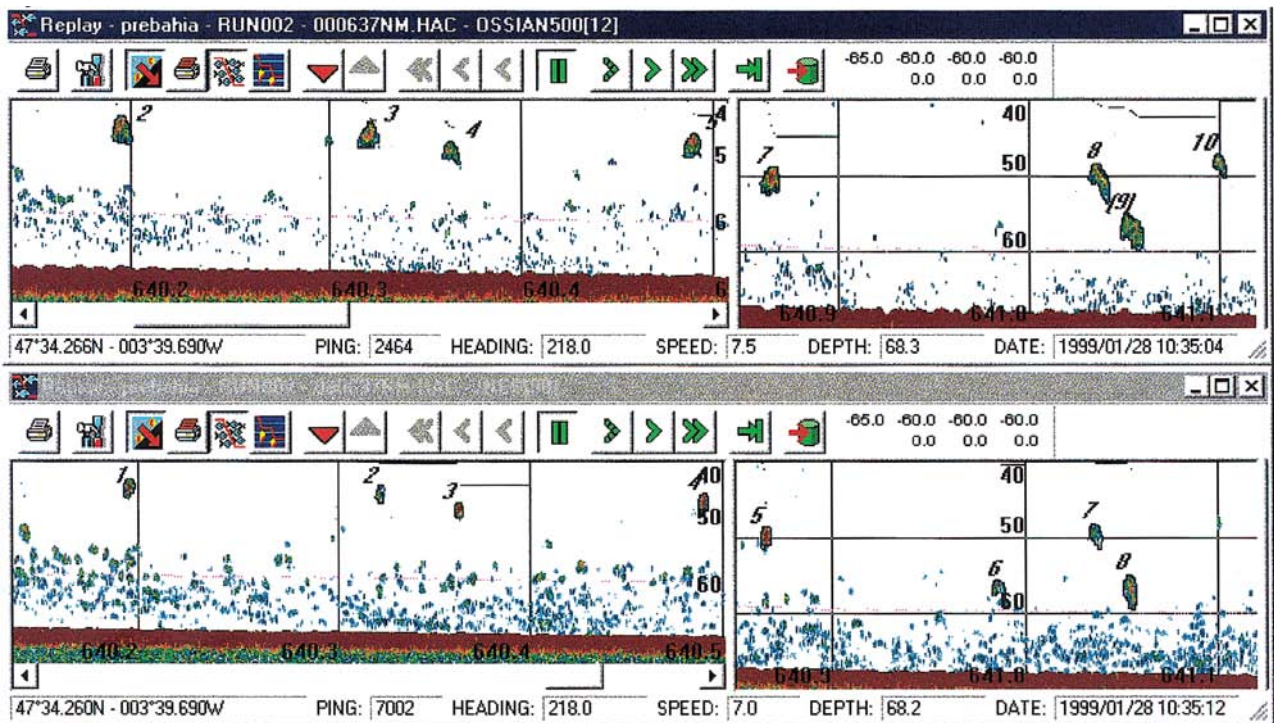


**Figure 12.** Compared echotracings at 12 kHz and 16° nominal angle (upper part) and 38 kHz and 5.7° nominal angle (lower part) obtained on small schools.

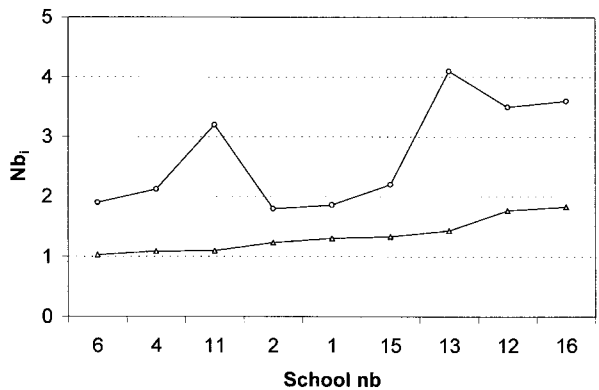


**Figure 13.** Compared  $Nb_i$  values for 12 kHz,  $16^\circ$  ( $\Delta$ ), and 38 kHz,  $5.7^\circ$  ( $\circ$ ) for different small schools, sorted by increasing values ( $16^\circ$ ). In this last case, the narrower beam gives  $Nb_i$  values greater than for  $16^\circ$ , inducing then better corrections for length and  $Sv$ . However, for schools No. 11 and 13, there are some strange differences.

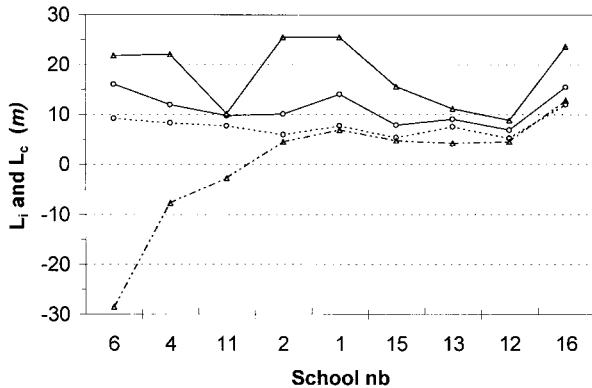


**Figure 14.** Compared image (continuous lines) and corrected (dotted lines) length for small schools for 12 kHz,  $16^\circ$  ( $\Delta$ ) and 38 kHz,  $5.7^\circ$  ( $\circ$ ). The different schools are arranged in ascending order for  $Nb_i$   $16^\circ$  factor.

beam width (factor  $Nb_i$ ). It then appears interesting to study the validity of the corrections comparatively for the two very different directivities:  $5.7^\circ$  and  $16^\circ$ . The types of echotracés used for this part are displayed in figure 12, and table III gives their main characteristics. Here,  $Nb_i$  numbers are generally small and in many cases for the directivity of  $16^\circ$  it was not possible to operate the correction algorithm.

The compared  $Nb_i$  values for  $5.7^\circ$  and  $16^\circ$  are plotted in figure 13 and some abnormal variations for school No. 11 and 13 can also be observed for these little traces by comparing the two frequency  $Nb_i$ .

In figure 14, concerning the lengths for school No. 2 and the others on the right part, where  $Nb_i$  is above 1.23 for  $16^\circ$  (and 1.8 for  $5.7^\circ$ ), the correspondence between corrected lengths is better. The algorithm limits appear clearly on this point: bad corrections –

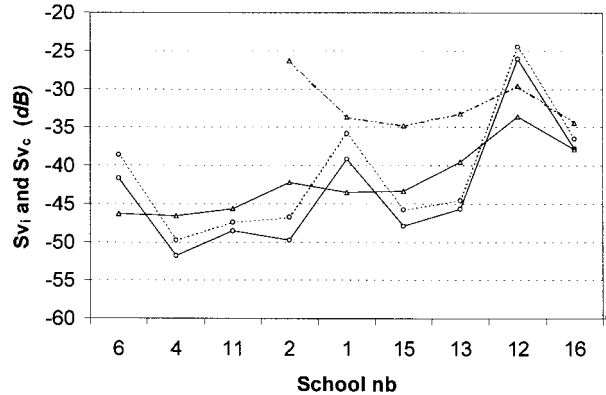


**Figure 15.** Compared image (continuous lines) and corrected (dotted lines)  $Sv$  of small schools for 12 kHz,  $16^\circ$  ( $\Delta$ ) and 38 kHz,  $5.7^\circ$  ( $\circ$ ). For schools No. 6 to 11 on the left part, there is no corrected value for  $16^\circ$ : these schools are too small comparatively to the beam and the corrections give negative values for length and no possibility to calculate  $Sv$  correction.

negative lengths – can even be obtained for echotracés whose lengths are too small compared to the beam width.

Figure 15 gives the compared corrections concerning  $Sv$ . As for the other cases above, the corrections concerning this parameter are not as accurate as those for length. For the smaller schools, it was impossible to calculate corrections using the  $16^\circ$  directivity. In this case, by comparison with the  $5.7^\circ$ -corrected values, which must be most accurate than the  $16^\circ$  one, it appears that the image values are not so bad (cf. suggested algorithm – step 2, section 2.5.2.4).

## 5. CONCLUSION

This practical exercise on real echotracés was necessary for a better investigation of the algorithm validity, designed to bring corrections for the descriptors extracted. Of course, in this case the corrections do not seem to offer the same level of accuracy as that reached on simulated data. This is mainly due to the variability encountered in the echotracés, resulting from complex shapes and varying internal densities.

The comparison between two very different directivities –  $16^\circ$  and  $5.7^\circ$  – was not always easy to operate, as the equipment gives different echotracés. Nevertheless, this practical exercise has demonstrated that:

- the use narrow beam echosounders is recommended: in this way, a greater number of traces can be processed with an acceptable accuracy,
- corrections concerning length appear quite often more accurate than those for volume backscattering strength,
- it is always necessary to observe the  $Nb_i$  values: when they are lower than 1.5, the accuracy is diminished and the algorithm must not be operated.

Echotraces shape and density can be modified by echosounder characteristics or school depth: the same school can be represented by very different images. Before conducting classification on the echotraces, it seems thus necessary to operate some corrections on the morphological or energetic descriptors that are commonly extracted in order to describe the kind of encountered concentration and to conduct classification works.

A special algorithm has been developed for this purpose. Based on simulated data, it generally gives good results when comparing the descriptors values extracted from both original and image schools. Nevertheless, the correction accuracy decreases deeply when the echotrace length is too small compared to the effective detection beam width:  $Nb_i$  value. When  $Nb_i$  is lower than 1.5, the algorithm must not be operated.

The simulated schools do not reflect the field variability: only ellipsoid shapes and uniform densities are studied. It was thus necessary to operate corrections on at-sea detection. In this case, even if quite fair results have been obtained, the accuracy was not at the same level than that reached on simulated data. This was mainly due to complex school morphology or varying internal density. This kind of exercise must be continued on many other examples for a better understanding of the phenomenon.

However, it can be concluded that:

- Corrections of school descriptors values are necessary for a better understanding of the field concentrations.
- An acceptable level of accuracy is reached when the echotraces length are large enough compared to the beam width ( $Nb_i > 1.5$ ); if  $Nb_i$  is less than 1.5, this kind of correction must not be done. Using narrow beam echosounders thus offers the possibility to accurately process a greater number of echotraces.
- For common school densities encountered for instance in the Bay of Biscay, processing thresholds

between  $-60$  and  $-65$  dB give  $dST$  value greater than 10 dB and the best chance of accuracy in correction.

- On field data, correction for length appears to be better than for density, and complex shape or density may be sources of inaccuracy.

## References

- Aglen, A., 1982. Echo-integrator threshold and fish density distribution. Symposium on Fisheries acoustics, Bergen. FAO Fish. Rep. No. 300, pp. 35–44.
- Diner, N., Scalabrin, C., 1997. Shoal acoustic image simulation. FAST Working Group, Hamburg.
- Johannesson, K.A., Losse, G.F., 1977. Methodology of acoustic estimations of fish abundance in some UNDP/FAO resource survey projects. Rapp. P-V. Cons. Int. Explor. Mer 170, 296–318.
- Olsen, K., 1969. A note on estimating school size from echotraces. FAO Fish. Rep. 78, 37–48.
- Reid, D.G., 2000. Report on echotrace classification. ICES Coop. Res. Rep., 238, III.
- Scalabrin, C., Massé, J., 1993. Acoustic detection of the spatial and temporal distribution of fish shoals in the Bay of Biscay. Aquat. Living Resour. 6, 269–283.
- Scalabrin, C., 1997. Identification acoustique des espèces pélagiques à partir d'attributs discriminants de bancs de poissons monospécifiques, Thèse de doctorat, océanographie biologique. Université de Bretagne occidentale, Brest.
- Soud, P., 1988. Automatisation de la description et de la classification des détections acoustiques de bancs de poissons pélagiques pour leur identification, Thèse de doctorat. Université Aix-Marseille-II, Marseille.
- Weill, A., Scalabrin, C., Diner, N., 1993. MOVIES-B: an acoustic detection description software. Application to shoal species classification. Aquat. Living Resour. 6, 255–267.